

**Magnetic anisotropy in epitaxial Mn<sub>5</sub>Ge<sub>3</sub> films**A. Spiesser,<sup>1,\*</sup> F. Viot,<sup>2</sup> L.-A. Michez,<sup>1,†</sup> R. Hayn,<sup>2</sup> S. Bertaina,<sup>2</sup> L. Favre,<sup>2</sup> M. Petit,<sup>1</sup> and V. Le Thanh<sup>1</sup><sup>1</sup>*Aix Marseille Université, CNRS, CINaM-UMR 7325, 13288 Marseille, France*<sup>2</sup>*Aix-Marseille Université, CNRS, IM2NP-UMR 7334, 13397 Marseille, France*

(Received 12 January 2012; revised manuscript received 12 July 2012; published 30 July 2012)

High crystalline quality Mn<sub>5</sub>Ge<sub>3</sub> films with thicknesses ranging 4–200 nm have been grown on Ge(111) substrates by solid phase epitaxy. The basal hexagonal plane of Mn<sub>5</sub>Ge<sub>3</sub> is in epitaxy with the Ge(111) plane. Magnetic properties of the films have been investigated as a function of the film thickness and the magnetization curves have been analyzed using a theory that includes a description of magnetic domains in uniaxial thin films. The results clearly indicate the existence of a critical thickness below which the magnetic stripe phase disappears. We have determined the value of this thickness to lie between 10 and 25 nm from the analysis of experimental magnetization curves and the theoretical fit of the in-plane remanent magnetization. Although analogies can be drawn between the behavior observed in our system and that of hcp Co, we have shown that the critical thickness is considerably smaller in Mn<sub>5</sub>Ge<sub>3</sub>; this has the potential to open new fields of applications for Mn<sub>5</sub>Ge<sub>3</sub> thin films in magnetic recording and spintronics.

DOI: [10.1103/PhysRevB.86.035211](https://doi.org/10.1103/PhysRevB.86.035211)

PACS number(s): 75.50.Cc, 75.60.–d, 75.30.Gw

**I. INTRODUCTION**

As device miniaturization reaches technological limits,<sup>1</sup> adding spin degree of freedom to the electron into conventional electronics appears as a promising solution. One approach to develop such spin-based devices relies on the ability to electrically inject spin-polarized carriers from ferromagnetic materials into semiconductors. Research dealing with group-IV semiconductors represents a particular interest since it allows us to integrate spintronics devices into the existing Si technology. Germanium, thanks to its small band gap and its high mobility, is believed to lead to a new generation of devices having high-speed data processing, high-density integration, and low power consumption.<sup>2</sup> In addition, its long spin coherence time is of great advantage for innovative spintronic devices. Recently the injection of a spin polarized current into Ge through a tunnel junction<sup>3–5</sup> has been successfully demonstrated. However, avoiding the insulating layer between the Ge and the ferromagnet (FM) will be required for the realization of gate-tunable spin devices.<sup>6</sup> Therefore achieving epitaxial growth of high quality FM directly on Ge is an important challenge for the development of spin electronics.

Materials with perpendicular magnetic uniaxial anisotropy are of particular interest<sup>7</sup> because of their applications in both emerging spintronics and next-generation data-storage technologies. Among them, Co and Co-based alloys such as CoPt are the most prominent candidates. However, their direct growth onto Ge is hindered by the fact that they are prone to form germanides at the interface that are not ferromagnetic. In this context, the ferromagnetic compound Mn<sub>5</sub>Ge<sub>3</sub> is an appealing candidate because it is possible to grow high quality epitaxial layers directly onto Ge.<sup>8</sup> Furthermore, its Curie temperature (296 K) can greatly be enhanced by carbon addition<sup>9</sup> and the resulting materials were shown to display remarkable thermal stability.<sup>10</sup> Finally, its high spin polarization<sup>11</sup> has potential for spin-based devices. During the last decades, the physical properties of this compound have been largely investigated.<sup>8,12–14</sup> In a recent paper,<sup>15</sup> we have shown that for a film thickness smaller than 10 nm, the shape of the hysteresis loops measured in plane and out of plane clearly

indicated that the direction perpendicular to the film surface is a hard axis and the easy axis of magnetization lies in the hexagonal basal (001) plane. When increasing the film thickness, the squareness of the in-plane hysteresis loop was found to decrease and the magnetic field required to saturate increased. However, due to a lack of experimental data, in particular in the small range of film thicknesses, the behavior of the magnetic anisotropy of the films could not be fully determined and the film thickness at which a transition from the in-plane to the out-of-plane magnetizations occurs still needs to be found out.

In this paper, we report a systematic study of magnetic properties of high quality Mn<sub>5</sub>Ge<sub>3</sub> with a thickness ranging from 4 to 200 nm. In particular, we have focused on the magnetic properties of films with thicknesses below 25 nm. We clearly demonstrate that the magnetization direction changes from in-plane for very thin films to a multidomain structure with out-of-plane direction for thicker samples. The hysteresis curves for a 16-nm-thick layer already show evidence of a magnetic reorientation along the *c* axis, proving that the critical thickness for the transition is below 20 nm. Moreover, for a 25-nm-thick layer a clear signature of a multidomain structure with perpendicular orientation is visible. All the results are supported by an improved version of Kittel's model for stripe domains that includes an accurate description of domain walls and accounts for the influence of the layer thickness on the magnetostatic energy. Despite analogies between the magnetic behavior observed in our system and that of hcp cobalt thin films, some noticeable differences are pointed out. In particular, the critical thickness in Mn<sub>5</sub>Ge<sub>3</sub> is much smaller than that of Co,<sup>16</sup> which opens new domains of applications for Mn<sub>5</sub>Ge<sub>3</sub> thin films in magnetic recording or spintronics.

**II. EXPERIMENTAL DETAILS**

Mn<sub>5</sub>Ge<sub>3</sub> films with thicknesses ranging 4–200 nm were grown onto Ge(111) substrates in a molecular beam epitaxy (MBE) system with a base pressure less than 10<sup>–10</sup> Torr. Before deposition, the substrates were chemically and thermally cleaned as explained in Refs. 17 and 15. The films were

grown via solid phase epitaxy (SPE), which consists of depositing Mn at room temperature and then annealing at 450 °C to activate interdiffusion and phase nucleation. We systematically checked the Mn deposition rate with a quartz crystal microbalance before starting the growth whereas Ge flux was determined from reflection high-energy electron diffraction (RHEED) intensity oscillations.

$\text{Mn}_5\text{Ge}_3$  growth was monitored *in situ* using a RHEED technique and Auger electron spectroscopy (AES). We performed structural analyses of post-grown films by means of high-resolution transmission electron microscopy (HRTEM) using a JEOL 3010 microscope operating at 300 kV with a spatial resolution of 1.7 Å. TEM enables us to directly measure the overall alloy thickness after annealing, which is proportional to the amount of Mn deposited and the nominal concentration of  $\text{Mn}_5\text{Ge}_3$ . The average value and the associated error bar that we report in this paper were determined from a set of different images taken on the same sample. The thickness dispersion originates from the surface roughness of the film, which increases with thickness. Typical growth conditions determined that the roughness is less than 1 nm for thin film ( $\leq 40$  nm) and about 3 nm for thicker epilayers. Magnetic properties of the films were probed with a Quantum Design superconducting quantum interference device (SQUID) magnetometer and for all the results reported in this paper, the diamagnetic contribution coming from the Ge substrate has been subtracted leaving only the magnetic signal coming from the  $\text{Mn}_5\text{Ge}_3$  films.

### III. RESULTS AND DISCUSSION

#### A. Structural characterizations

We monitored surface structures of the grown films using RHEED. The observed patterns are identical throughout the range of thicknesses that we studied; they show a smooth surface with a  $(\sqrt{3} \times \sqrt{3})R30^\circ$  reconstruction, as shown in the inset of Fig. 1 of Ref. 15. This can be unambiguously attributed to the growth of  $\text{Mn}_5\text{Ge}_3$  on Ge(111) with both the [120] axis of the alloy parallel to the  $[1\bar{1}0]$  axis of the Ge substrate and the  $c$  axis of the hexagonal structure of  $\text{Mn}_5\text{Ge}_3$  perpendicular to the Ge(111) plane.<sup>17</sup> We confirmed these epitaxial relationships by HRTEM measurements. For thin films, which are defined as less than a few tenths of nm, HRTEM images reveal a heterostructure of very high crystalline quality with an atomically sharp interface, as shown in the case of a 4.5-nm-thick epilayer [Fig. 1(a)]. As the film becomes thicker, the interface and the upper surface become a bit rougher; this is demonstrated by a 170-nm-thick  $\text{Mn}_5\text{Ge}_3$  film grown onto Ge(111) in Fig. 1(b). However, HRTEM images taken near the interface still reveal a high crystal quality [Fig. 1(c)]. X-ray-diffraction (XRD) scans (not shown here) display only the (0002) and (0004) reflections of the  $\text{Mn}_5\text{Ge}_3$  corresponding to the bulk parameters. No residual Mn can be detected, which means that all the deposited Mn has reacted to form a new single phase. Surprisingly, diffraction due to other phases was not observed in our measurements despite the fact that  $\text{Mn}_5\text{Ge}_3$  is not the most stable phase of Mn-Ge diagram. This peculiar behavior comes from similarities between the crystallographic symmetries of the Ge(111) substrate and the

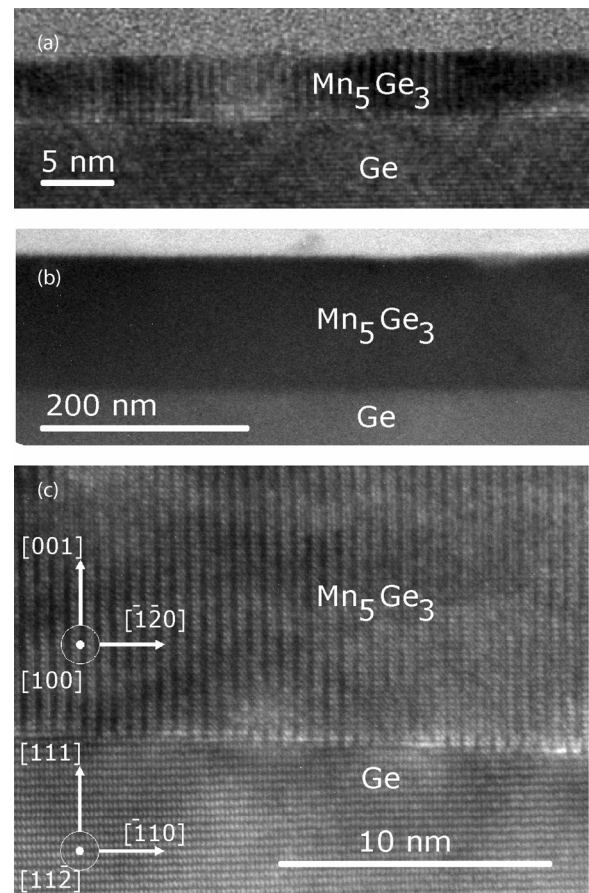


FIG. 1. (a) and (b) correspond to TEM images of a 4.5- and a 168-nm-thick samples, respectively. (c) HRTEM cross section of the interface between a 168-nm-thick  $\text{Mn}_5\text{Ge}_3$  layer and the Ge substrate.

$\text{Mn}_5\text{Ge}_3$  layer, which leads to the stabilization of the hexagonal structure; this occurs despite the 3.7% lattice mismatch to the detriment of the orthorhombic  $\text{Mn}_{11}\text{Ge}_8$  compound.

Another noteworthy point to discuss is the strain relaxation state: from the measurements of the distance between the RHEED streaks, the film appears totally relaxed even for layers as thin as 1 nm.<sup>15</sup> This result differs slightly from recent results where a partial strain in a 3.3-nm-thick  $\text{Mn}_5\text{Ge}_3$  film grown in similar conditions<sup>18</sup> has been detected. However, it is surprising that in both cases, no clear defects, which should be induced by the relaxation phenomenon, are visible in TEM images. After a systematic investigation of all the analyzed samples, only misfit point defects are observed (Ref. 15). However, threading dislocations are absent in our films. This behavior may be attributed to the high value of the elastic modulus of  $\text{Mn}_5\text{Ge}_3$ , which is 110 GPa compared to 77.2 GPa for Ge, allowing  $\text{Mn}_5\text{Ge}_3$  films to deform elastically on Ge.

#### B. Magnetic properties

A systematic study of the magnetic properties of  $\text{Mn}_5\text{Ge}_3$  has been carried out as a function of film thicknesses using a SQUID magnetometer. We measured the saturation magnetic moment normalized by the surface area and plotted this as a function of the film thickness, as shown in Fig. 2. The expected linear behavior<sup>19</sup> is directly related to the intrinsic

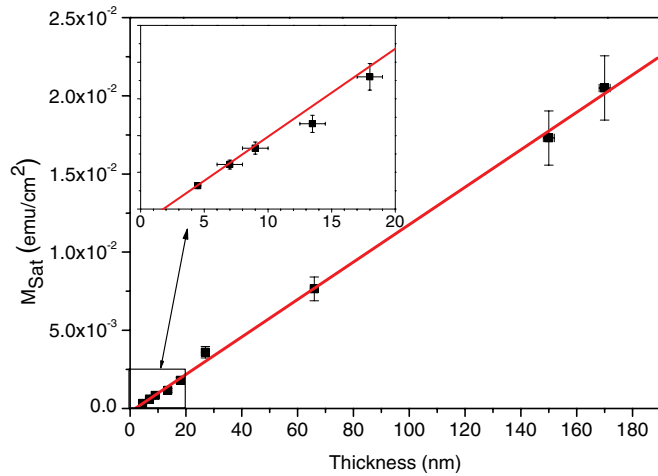


FIG. 2. (Color online) Saturation magnetic moment per surface area as a function of the film thickness. The slope of the linear fit gives the intrinsic magnetization of  $\text{Mn}_5\text{Ge}_3$ .

magnetization of  $\text{Mn}_5\text{Ge}_3$  that has been determined to be  $M = 1200 \pm 150 \text{ emu/cm}^3$ . This value is very close to the bulk quoted value of  $1070 \text{ emu/cm}^3$  obtained experimentally<sup>20</sup> and theoretically.<sup>11</sup> The extrapolation of the linear fit to zero magnetization gives a non-null thickness, which points to the presence of a ferromagnetically dead layer (FDL) of about  $1.7 \pm 0.3 \text{ nm}$ , thus reducing the active magnetic volume. In the following part, the thicknesses used for the magnetization calculations (Figs. 3 and 5) correspond to the magnetically active volume of the  $\text{Mn}_5\text{Ge}_3$  film and are defined as the measured thicknesses deduced from the TEM images minus the FDL thickness. The presence of a dead layer could partly explain the very low magnetization in a recent study reporting magnetic properties of a 3.3-nm-thick  $\text{Mn}_5\text{Ge}_3$  film.<sup>18</sup> Other systems show similar behavior.<sup>21–23</sup> For example, in the Co/Ge(111) heterostructure, the critical thickness leading to the paramagnetic-ferromagnetic transition lies between 5 and  $8 \text{ \AA}$ .<sup>24</sup> Such a magnetic dead layer could result from various phenomena: interdiffusion and formation of an interfacial alloy that is generally not ferromagnetic,<sup>21,22,25</sup> interfacial roughness,<sup>23</sup> proximity of a nonmagnetic material,<sup>26</sup> and strain at the interface.<sup>27</sup> Here, the structural and magnetic analyses do not allow us to determine precisely the origin of the FDL. Further studies will be required to understand this phenomenon. However, the effect of the annealing temperature<sup>25</sup> and incorporation of doping elements at the interface may lead to solutions for decreasing the dead layer thickness.

Hysteresis ( $M$ - $H$ ) loops measured with the magnetic field applied parallel and perpendicularly to the sample plane are displayed in Fig. 3. Among all the measured samples, only results for 7-, 16-, 25-, 64- and 168-nm-thick films are shown because they resume very well the evolution of the magnetic properties. Insets represent a zoom around the positive saturation field of the out-of-plane configuration. Parallel and perpendicular configurations for thick samples lead apparently to similar magnetic reversal; this is surprising since we expect an easy magnetization axis along the  $c$  axis, which is perpendicular to the sample plane. Previous work<sup>15</sup> has already reported a similar trend, which suggests

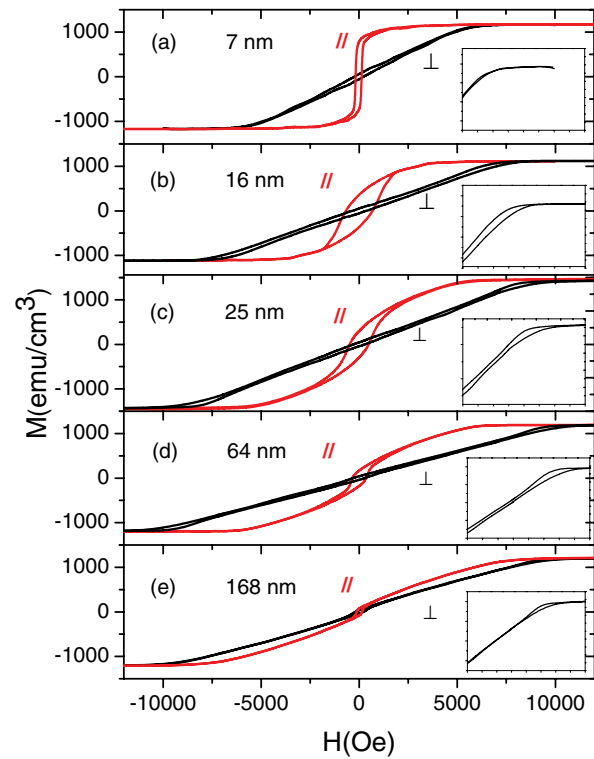


FIG. 3. (Color online) Magnetic hysteresis curves with the external magnetic field applied in the sample plane and perpendicular to it for different thicknesses of  $\text{Mn}_5\text{Ge}_3$  films: (a) 7 nm; (b) 16 nm; (c) 25 nm; (d) 66 nm; (e) 168 nm. Insets zoom to the positive field branch (from 4000 to 12000 Oe) of the perpendicular configuration. All the measurements have been done at 15 K.

that the magnetization easy axis leaves the in-plane direction. However, no clear description of the magnetic behavior as a function of thickness has been proposed.

We observe a steady change in the magnetic behavior of in-plane  $M$ - $H$  curves in Fig. 3. For samples thinner than 10 nm, the hysteresis loop exhibits a square shape that unambiguously shows that the magnetization easy axis lies in-plane. For thicker samples, the  $M$ - $H$  curves become increasingly canted as the saturation field increases with thickness but a hysteresis is still visible around zero field. In the out-of-plane configuration, at first sight, the hysteresis loops appear similar throughout the range of the studied thicknesses: little hysteresis is present and the saturation fields are higher than the ones observed in the parallel configuration. In Fig. 4, we summarize the variation of the perpendicular saturation field as a function of the film thickness. Two regimes can clearly be distinguished: first, below thicknesses of about 20 nm, the perpendicular saturation field increases rapidly with the film thickness; second, above this thickness, it is independent of the film thickness and fluctuates around  $10000 \pm 1000 \text{ Oe}$ . More importantly, the general shape of the hysteresis curves changes. Above a threshold thickness, a singularity in all the out-of-plane  $M$ - $H$  curves appears around the saturation field as demonstrated in the inset of Fig. 3(c) for a 25-nm-thick sample. By describing the  $M$ - $H$  curve from positive saturation to lower field values, a characteristic opening of the hysteresis loop appears around the saturation field over a narrow range

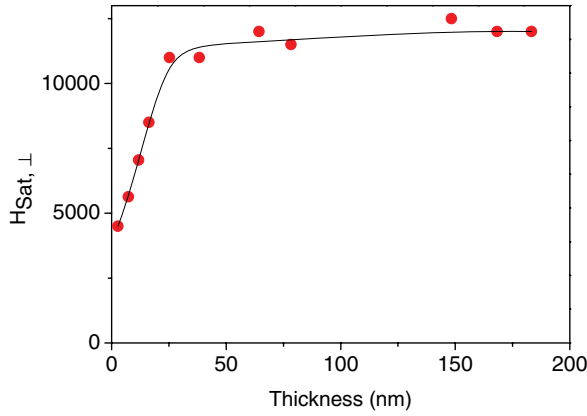


FIG. 4. (Color online) Out-of-plane saturation field as function of thickness. The solid line serves as a guide for the eye.

of fields. As the field decreases, the two  $M$ - $H$  branches return to a similar field dependence and this singularity disappears. This feature is not present in hysteresis loops of layers thinner than 10 nm where the magnetization rises linearly with the applied field and almost reversibly. In this latter case, the magnetostatic energy is the dominating term forcing the magnetization to lie in the sample plane in a monodomain structure. As the film thickness increases, the contribution of the magnetocrystalline energy grows. Since bulk  $\text{Mn}_5\text{Ge}_3$  exhibits uniaxial anisotropy along the  $c$  axis,<sup>28</sup> we expect a reorientation of the magnetization from the in-plane to the out-of-plane direction as it occurs in very similar systems: for example, in epitaxial (0001) hcp cobalt films grown on ruthenium,<sup>16</sup> magnetic domains with perpendicular anisotropy are formed above a critical thickness of 50 nm. The comparison between the shape of the magnetization curves for the two systems is striking and suggests the presence of a stripe domain structure in  $\text{Mn}_5\text{Ge}_3$  films at least thicker than 25 nm. The singularity in the magnetization curves in the perpendicular configuration can indeed be attributed to sudden nucleation of magnetic domains with opposite magnetization<sup>29,30</sup> while the remanence in the in-plane magnetization curves originates from the magnetization reversal at the center of the wall. In the  $\text{Mn}_5\text{Ge}_3$  system, the magnetization reorientation from fully in plane to fully out of plane occurs therefore between 10 and 25 nm; as a matter of fact, the 16-nm-thick film depicts an intermediate regime with a slight opening of the  $M$ - $H$  curve over a range of fields comprised between the two saturation fields. We emphasize that this critical value is much smaller than the predicted value for that material.<sup>12</sup>

### C. Theoretical model

To fully explain the experimental results, we have developed a theory that can both predict the critical thickness and describe some characteristic features of the  $M$ - $H$  curves above this value. Our model of stripe domains improves upon the model described by Kittel.<sup>31</sup> It includes a good description of the domain walls while taking into account the magnetostatic interaction between top and bottom surfaces (for more details see Ref. 32). The magnetization in the domains is assumed to be constant and is equal to the saturation magnetization. In magnetic films with a stripe-domain structure, the size of

oppositely magnetized domains is a basic parameter; therefore a period corresponds to two adjacent domains with their associated domain walls. The latter are assumed to be of Bloch type with a magnetization profile of cosinelike form. Such a description of the domain-wall profile has been already used by Yafet and Gyorgy in Ref. 33. However, they can analyze the magnetostatic energy only for a thickness that is much smaller than the domain width. Our model is not limited to this restriction. The total energy of this new system can be written as

$$E_{\text{tot}} = \frac{4d}{t} \sum_{k=1, \text{odd}}^{\infty} \left( \frac{|C_k|^2}{k} * (1 - e^{-\pi kt/d}) \right) + \frac{\pi^2}{d\delta} A + \frac{\delta}{2d} K, \quad (1)$$

where  $C_k = \frac{2M_0}{k\pi[1-k^2(\frac{\delta}{d})^2]} \cos[k\pi \frac{\delta}{2d}]$ .

The first term of Eq. (1) represents the magnetostatic energy and has been calculated using the analogy with the electrostatic field for alternating (positive and negative) charged stripes.<sup>34</sup>  $d$ ,  $\delta$ , and  $t$  represent the half period, the wall width, and the thickness, respectively. The domain width can be simply deduced and is equal to  $d - \delta$ . The magnetization in the inner domain is denoted by  $M_0$ . The second term represents the exchange energy where  $A$  is the exchange constant while the last term corresponds to the magnetocrystalline energy wherein  $K$  is the uniaxial anisotropy constant. The cosinelike form of the wall gives a good approximation of the magnetization profile obtained by the variational method. Contrary to Kittel's model,<sup>31</sup> which neglects the domain wall in the magnetostatic energy, one can extract the in-plane remanent magnetization due to the wall. If a small magnetic field is applied in the film plane, the magnetic moment of each domain wall is parallel to the in-plane field direction with all moments pointing in the same sense. When the magnetic field tends to zero it is easy to calculate the remanent magnetization that corresponds to only the in-plane contribution of the domain wall. The cosinelike form of wall leads to the following expression:

$$\frac{M_r}{M_0} = \frac{1}{d} \int_0^{\delta} \sin \frac{\pi x}{\delta} dx = \frac{2\delta}{\pi d}. \quad (2)$$

To test if the stripe model picture can be applied to describe the experimental results of  $\text{Mn}_5\text{Ge}_3$ , we fitted the in-plane remanent magnetization. The magnetocrystalline constant ( $K$ ) is extracted from experimental measurements<sup>28</sup> at 77 K and is extrapolated to 15 K; it equals to  $4.3 \times 10^6$  erg/cm<sup>3</sup>. The exchange ( $A$ ) and saturation magnetization ( $M_0$ ) constants, however, are taken as adjustable parameters. The best fit is shown in Fig. 5; it gives an exchange constant equal to  $1 \times 10^{-7}$  erg/cm, which is a reasonable value and a saturation magnetization equal to 1040 emu/cm<sup>3</sup>. The latter value agrees well with all experimental measurements. It has to be noted that the exchange constant is considerably smaller than in hcp Co, which also explains the smaller critical thickness in the present case.

The critical thickness for which the magnetization flips from the out-of-plane to the in-plane direction corresponds to the situation where the domain width tends towards zero and the total energy equals  $K$ . From the plot of the variation of the half period and the wall width as a function of the film thickness

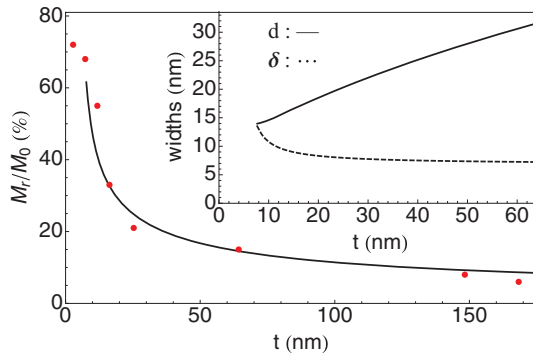


FIG. 5. (Color online) In-plane remanence as a function of thickness. The best fit (full line) to the experimental measurements (points) has been found for an exchange constant equal to  $1 \times 10^{-7}$  erg/cm and a saturation magnetization equal to  $1040 \text{ emu/cm}^3$ . The inset depicts the behavior of half period (full line) and wall (dashed line) widths as a function of thickness. Calculations use parameters obtained for the best fit of the in-plane remanence as a function of thickness.

shown in the inset of Fig. 5, it has been estimated to 8 nm. This is a lower bound of the critical thickness extracted from the magnetization curves (Fig. 3) but it is also confirmed by the theoretical analysis of the in-plane remanent magnetization. Below this value, the magnetic configuration is an in-plane monodomain structure whereas above it, a multidomain structure appears due to the high magnetocrystalline constant compared to the magnetostatic term. Interestingly, both critical thickness and minimum domain size are much smaller in  $\text{Mn}_5\text{Ge}_3$  than in any conventional uniaxial thin films. As it can be seen in the inset of Fig. 5, the model predicts that the domain wall's width first decreases rapidly with the film thickness and from a thickness of about 20 nm the domain wall's size varies only slightly with the thickness. This trend is in good agreement with the evolution of the perpendicular saturation field (Fig. 4), which synthesizes very well the overall behavior. Up to a thickness of about 20 nm, the in-plane

contribution of the walls varies, resulting in an increase of the perpendicular saturation field. From this thickness, only the size of the domains changes and the perpendicular saturation field keeps constant. In comparison, a thickness of a few hundreds of nm is required in Co to saturate the perpendicular saturation field.<sup>35</sup> It is also worth noting that the minimum value of a half period in cobalt is four times higher than that in  $\text{Mn}_5\text{Ge}_3$ . Furthermore, this value increases more slowly with thickness in the case of  $\text{Mn}_5\text{Ge}_3$ . As a result, domain sizes in  $\text{Mn}_5\text{Ge}_3$  should be much smaller in  $\text{Mn}_5\text{Ge}_3$  than in any conventional uniaxial thin films and could be controlled by the film thickness, which could place  $\text{Mn}_5\text{Ge}_3$  as a potential candidate for new-generation data-storage devices.

#### IV. CONCLUSION

In this paper we use conventional magnetometric measurements to study the reorientation of the magnetization in thin  $\text{Mn}_5\text{Ge}_3$  films from in plane to out of plane. We have shown that this transition occurs for a film thickness lying between 10 and 25 nm. This result is strongly supported by theoretical calculations based on an improved version of Kittel's model, which is better suited to retranscribe the magnetic behavior of domains in uniaxial thin films. We point out that this critical thickness is much smaller in  $\text{Mn}_5\text{Ge}_3$  than in any conventional uniaxial thin film. From our calculations, the size of magnetic domains in  $\text{Mn}_5\text{Ge}_3$  may also be considerably smaller than the one in any other known magnetic system. Furthermore, these domains can be tailored by the film thickness. The characteristics described in this paper highlight the potential applicability of  $\text{Mn}_5\text{Ge}_3$  thin films, especially for the next generation of data-storage devices and the Si-Ge spin-based electronics.

#### ACKNOWLEDGMENTS

We would like to acknowledge ANR MnGe-Spin for funding and M. Kuzmin for helpful discussions.

\*Present address: AIST, Tsukuba, Ibaraki 305-8568, Japan.

†michez@cinam.univ-mrs.fr

<sup>1</sup>International Technology Roadmap for Semiconductors (ITRS), 2009 Edition, Emerging Research Materials, [www.itrs.net](http://www.itrs.net).

<sup>2</sup>G. Scappucci, G. Capellini, B. Johnston, W. M. Klesse, J. A. Miwa, and M. Y. Simmons, *Nano Lett.* **11**, 22721 (2011).

<sup>3</sup>H. Saito, S. Watanabe, Y. Mineno, S. Sharma, R. Jansen, S. Yuasa, and K. Ando, *Solid State Commun.* **151**, 1159 (2011).

<sup>4</sup>Y. Zhou, W. Han, L.-T. Chang, F. Xiu, M. Wang, M. Oehme, I. A. Fischer, J. Schulze, R. K. Kawakami, and K. L. Wang, *Phys. Rev. B* **84**, 125323 (2011).

<sup>5</sup>A. T. Hanbicki, S.-F. Cheng, R. Goswami, O. M. J. van't Erve, and B. T. Jonker, *Solid State Commun.* **152**, 244 (2012).

<sup>6</sup>Y. Ando, K. Hamaya, K. Kasahara, Y. Kishi, K. Ueda, K. Sawano, T. Sadoh, and M. Miyao, *Appl. Phys. Lett.* **94**, 182105 (2009).

<sup>7</sup>J. M. Shaw, H. T. Nembach, and T. J. Silva, *Phys. Rev. B* **85**, 054412 (2012).

<sup>8</sup>C. Zeng, S. C. Erwin, L. C. Feldman, A. P. Li, R. Jin, Y. Song, J. R. Thompson, and H. H. Weitering, *Appl. Phys. Lett.* **83**, 5002 (2003).

<sup>9</sup>A. Spiesser, I. Slipukhina, M. T. Dau, E. Arras, V. Le Thanh, L. Michez, P. Pochet, H. Saito, S. Yuasa, M. Jamet, and J. Derrien, *Phys. Rev. B* **84**, 165203 (2011).

<sup>10</sup>A. Spiesser, V. Le Thanh, S. Bertaina, and L. A. Michez, *Appl. Phys. Lett.* **99**, 121904 (2011).

<sup>11</sup>S. Picozzi, A. Continenza, and A. J. Freeman, *Phys. Rev. B* **70**, 235205 (2004).

<sup>12</sup>R. Gunnella, L. Morresi, N. Pinto, R. Murri, L. Ottaviano, M. Passacantando, F. D'Orazio, and F. Lucari, *Surf. Sci.* **577**, 22 (2005).

<sup>13</sup>A. Stroppa and M. Peressi, *Phys. Status Solidi A* **204**, 44 (2007).

<sup>14</sup>A. Stroppa, G. Kresse, and A. Continenza, *Appl. Phys. Lett.* **93**, 092502 (2008).

<sup>15</sup>A. Spiesser, S. F. Olive-Mendez, M.-T. Dau, L. A. Michez, A. Watanabe, V. Le Thanh, A. Glachant, J. Derrien, A. Barski, and M. Jamet, *Thin Solid Films* **518**, S113 (2010).

<sup>16</sup>M. Hehn, S. Padovani, K. Ounadjela, and J. P. Bucher, *Phys. Rev. B* **54**, 3428 (1996).

<sup>17</sup>S. Olive-mendez, A. Spiesser, L. A. Michez, V. Le Thanh, A. Glachant, J. Derrien, T. Devillers, A. Barski, and M. Jamet, *Thin Solid Films* **517**, 191 (2008).

- <sup>18</sup>P. De Padova, J.-M. Mariot, L. Favre, I. Berbezier, B. Olivieri, P. Perfetti, C. Quaresima, C. Ottaviani, A. Taleb-Ibrahimi, P. Le Fevre, F. Bertran, O. Heckmann, M. C. Richter, W. Ndiaye, F. D’Orazio, F. Lucari, C. M. Cacho, and K. Hricovini, *Surf. Sci.* **605**, 638 (2011).
- <sup>19</sup>B. N. Engel, C. D. England, R. A. Van Leeuwen, M. H. Wiedmann, and C. M. Falco, *Phys. Rev. Lett.* **67**, 1910 (1991).
- <sup>20</sup>G. Fischer, G. Kappel, and A. Jaegle, *Phys. Lett. A* **45**, 267 (1973).
- <sup>21</sup>T. L. Monchesky and J. Unguris, *Phys. Rev. B* **74**, 241301 (2006).
- <sup>22</sup>S. Entani, M. Kiguchi, S. Ikeda, and K. Saiki, *Thin Solid Films* **493**, 221 (2005).
- <sup>23</sup>M. Li and G.-C. Wang, *J. Magn. Magn. Mater.* **217**, 199 (2000).
- <sup>24</sup>J. S. Tsay, Y. T. Chen, W. C. Cheng, and Y. D. Yao, *J. Magn. Magn. Mater.* **282**, 81 (2004).
- <sup>25</sup>J. S. Tsay, C. S. Yang, Y. Liou, and Y. D. Yao, *J. Appl. Phys.* **85**, 4967 (1999).
- <sup>26</sup>J. Tersoff and L. M. Falicov, *Phys. Rev. B* **26**, 6186 (1982).
- <sup>27</sup>M. Sirena, E. Kaul, M. B. Pedreros, C. A. Rodriguez, J. Guimpel, and L. B. Steren, *J. Appl. Phys.* **109**, 123920 (2011).
- <sup>28</sup>Y. Tawara and K. Sato, *J. Phys. Soc. Jpn.* **18**, 773 (1963).
- <sup>29</sup>J. A. Cape and G. W. Lehman, *J. Appl. Phys.* **42**, 5732 (1971).
- <sup>30</sup>N. Saito, H. Fujiwara, and Y. Sugita, *J. Phys. Soc. Jpn.* **19**, 1116 (1964).
- <sup>31</sup>C. Kittel, *Phys. Rev.* **70**, 965 (1946).
- <sup>32</sup>F. Viot, L. Favre, R. Hayn, and M. D. Kuz’min (unpublished), arXiv:1202.6162.
- <sup>33</sup>Y. Yafet and E. M. Gyorgy, *Phys. Rev. B* **38**, 9145 (1988).
- <sup>34</sup>L. D. Landau and E. Lifchitz, *Electrodynamics in Continuous Media*, Course of Theoretical Physics (Mir, Moscow, 1969), Vol. 8.
- <sup>35</sup>M. Hehn, K. Ounadjela, S. Padovani, J. P. Bucher, J. Arabski, N. Bardou, B. Bartenlian, C. Chappert, F. Rousseaux, D. Decanini, F. Carcenac, E. Cambril, and M. F. Ravet, *J. Appl. Phys.* **79**, 5068 (1996).